J. Biochem. 121, 29-37 (1997)

Rhodamine 800 as a Probe of Energization of Cells and Tissues in the Near-Infrared Region: A Study with Isolated Rat Liver Mitochondria and Hepatocytes

Jun Sakanoue,* Kazuhiko Ichikawa,* Yasutomo Nomura,† and Mamoru Tamura†,1

*Graduate School of Earth Environmental Science, and †Division of Biophysics, Research Institute for Electronic Science, Kita-ku, Hokkaido University, Sapporo 060

Received for publication, July 29, 1996

To examine the feasibility of optical monitoring of cellular energy states with tissue-transparent near-infrared (NIR) light, the absorption and fluorescence characteristics of Rhodamine 800 in isolated rat liver mitochondria and hepatocytes were investigated. When the dye was incubated with isolated mitochondria, a large red shift of the absorption spectra and quenching of the fluorescence intensity were observed. The absorbance difference at 730 minus 685 nm, or at 730 minus 800 nm, and the fluorescence intensity measured at 692 nm varied linearly with the mitochondrial membrane potential. The spectral changes observed could be explained in terms of the potential-dependent uptake of the dye from the buffer solution into the mitochondrial matrix. The respiration control ratio and oxygen consumption rate were not affected by the addition of Rhodamine 800 at concentrations lower than 5 μM, which was the concentration range mostly employed throughout the present study. In a suspension of hepatocytes, the red shift and fluorescence quenching of Rhodamine 800 characteristic of energized mitochondria were also observed, and these changed to those of the buffer solution with the addition of an uncoupler under normoxia. At the early stage of anoxia, within about 5 min, when cytochrome oxidase was completely reduced, hepatocytes were concluded to be in the fully energized state, since the optical characteristics of Rhodamine 800 were the same as those of energized mitochondria. On the basis of these *in vitro* data, Rhodamine 800 is concluded to be a possible NIR-active contrast agent, that can be used to monitor the energy states of living tissues, in addition to the tissue oxygenation states, by the use of near-infrared spectrophotometry (NIRS) without harmful effects.

Key words: fluorescence quenching, hepatocyte, mitochondrial energy state, NIRS, Rhodamine 800.

To optically probe the energy states of cells and tissues *in vivo* non-invasively, various fluorescence and absorption dyes have been examined. Among these dyes, several are accumulated in living cells, and their optical properties change markedly with changes in cellular energy states, such as membrane potential (*1-5*). For instance, Emaus *et al.* (*5*) reported that the absorption and emission spectra of Rhodamine 123, a cationic fluorescence dye, were shifted to longer wavelengths by uptake into the mitochondrial matrix. The degree of this red shift is energy-dependent and linearly related to the mitochondrial potassium diffusion potential. Based on these properties of Rhodamine 123, energy-selective optical staining of cells in tissue was performed by the use of fluorescence microscopy (*6*).

However, the application of this approach has been limited to isolated cells and mitochondria. It has not been employed for tissues with circulating blood since light in the ultraviolet-visible region is not transmitted through tissues more than 1 mm in thickness. In contrast, near-infrared light in the range from 700 to 1,300 nm can be transmitted through much thicker tissues, such as a baby's head around 10 cm in diameter (*7*). Consequently, near-infrared spectrophotometry has been developed extensively for non-invasive optical monitoring in clinical medicine, especially for oxygen monitoring of cerebral tissues (*8*). Several animal studies in which hemoglobin oxygenation state and redox state of cytochrome oxidase in cerebral tissues were measured under various respiration conditions have also been reported (*9-11*).

However, the application of NIRS is currently limited *in vivo*, since only hemoglobin, myoglobin, and cytochrome oxidase are measurable by this technique, which can report the oxygenation states of circulatory blood and tissues, but not other parameters such as the energy state of the tissue. These limitations could be overcome by the introduction of an energy-reporting contrast agent. We chose Rhodamine 800 (Fig. 1) (*12-16*) as a possible contrast agent active in the near- infrared region.

In this paper, we will report the optical characteristics of Rhodamine 800 incorporated into isolated mitochondria and hepatocytes. Absorbance changes and fluorescence

1 To whom correspondence should be addressed. Fax: +81-11-706-4964, Tel: +81-11-706-2410

Abbreviations: CCCP, carbonyl cyanide *m*-chlorophenylhydrazone; RCR, respiratory control ratio; NIRS, near-infrared spectrophotometry; DMSO, dimethyl sulfoxide.

changes measured at around 700-800 nm quantitatively reflected changes in the energy state and respiratory conditions. We consider that this dye has potential utility for optical diagnosis in clinical NIRS.

MATERIALS AND METHODS

Rat Liver Mitochondria—Mitochondria were isolated from the liver of male Wistar rats (body weight 200-300 g, starved overnight) by the standard procedure (*17*) and were suspended in 5 mM Tris-HCl buffer (pH 7.4) containing 0.25 M mannitol. Mitochondria having a respiratory control ratio (RCR) higher than 4 were used for the experiments. Protein concentration was determined by the method of Lowry *et al.* (*18*) using BSA as a standard.

Isolated Hepatocytes—Hepatocytes were isolated from liver of rats (starved overnight) by the collagenase perfusion method (*19*). The perfusate was modified Krebs-Ringer bicarbonate buffer equilibrated with 95% O_2+5% CO_2 at 37°C and pH 7.4. The reaction mixture contained 10 mM HEPES, 139 mM NaCl, 3.57 mM $NaHCO_3$, 5.63 mM KCl, 1.42 mM $MgSO_4$, 1.43 mM KH_2PO_4, and 3.03 mM $CaCl_2$. The cell viability was checked by the trypan blue exclusion test. Preparations with more than 90% intact cells were used for the experiments.

Oxygen Consumption Rates—Oxygen consumption rates of isolated mitochondria and hepatocytes were measured using a Clark-type oxygen electrode. For simultaneous measurements of oxygen consumption and spectrophotometric characteristics, a special optical cell, designed so that the electrode could be inserted into it, was used. Gentle stirring was performed in the spectrophotometer; it did not interfere with the optical measurements.

Spectrophotometric Measurements—Absorbance measurements were made with a conventional dual-wavelength spectrophotometer, Shimadzu UV-3000. Wavelength pairs for the measurements of Rhodamine 800 were 730-685 and 730-800 nm. Redox changes of mitochondrial cytochrome oxidase were followed by measurement of the absorbance change at 620-605 nm of the heme moiety. For simultane ous measurements of Rhodamine 800 and cytochrome oxidase, a two-channel dual-wavelength spectrophotometer with a rotating disc (Unisoku, Osaka) was also employed.

Fluorescence measurements were made with a fluorophotometer, Shimadzu RF-540. For the measurements of Rhodamine 800, the excitation wavelength was set at 660 nm, and a cutoff filter (Toshiba, R-68) was employed to avoid contamination by the excitation light. The measurements were carried out at 25 and 37°C for the mitochondrial suspension and hepatocytes, respectively.

Potassium Diffusion Potential—Potassium diffusion potential of the mitochondrial membrane was calculated by use of the Nernst equation (1).

$$\Delta\Psi_{K^+}(mV) = 59 \log ([K^+]_{in}/[K^+]_{out}) \quad (1)$$

where $[K^+]_{in}$ was assumed to be 120 mM (*20*).

Chemicals—Rhodamine 800 (Fig. 1) of laser grade was purchased from Lambda Physik (Germany). It was dissolved in dimethyl sulfoxide (DMSO) and the solution was stored at room temperature. Small amounts of the stored solution were dissolved in aqueous buffer solution or organic solvents as required. All the reagents used were of analytical grade.

RESULTS

Optical Characteristics of Rhodamine 800 in Various Solvents—Figure 2A shows the optical absorption spectra of Rhodamine 800 in various organic solvents and in aqueous solution in the visible and near-infrared regions. The absorption maximum at 683 nm in acetone shifted to 696 nm in DMSO without a significant change of the overall spectral profile. The spectrum in aqueous solution was intermediate between those in acetone and DMSO, though the absorption intensity became about half of that in acetone.

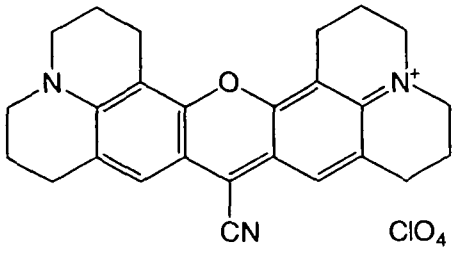

$C_{26}H_{26}N_3O_5Cl$

MW : 495.52

Fig. 1. **Chemical structure of Rhodamine 800.**

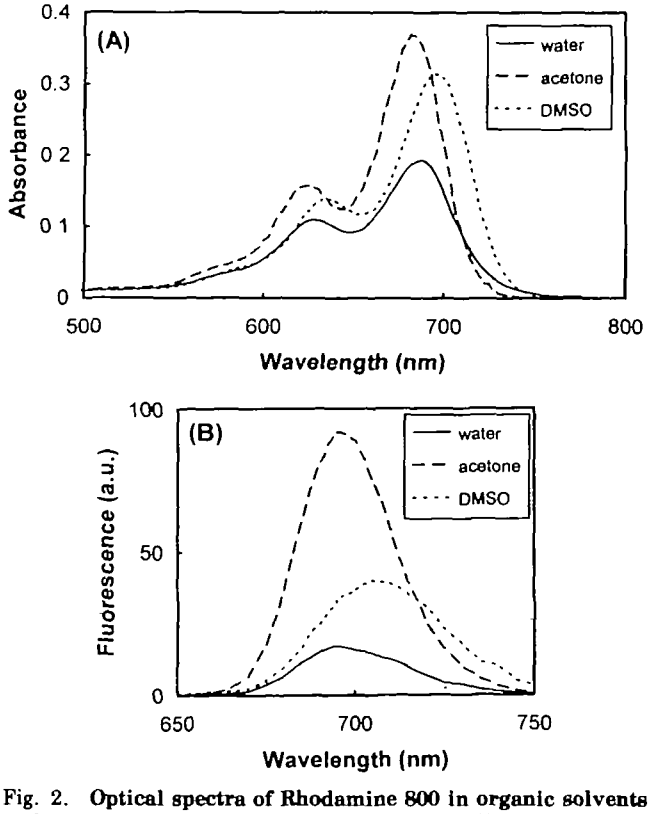

Fig. 2. **Optical spectra of Rhodamine 800 in organic solvents and water.** In absorbance (A) and fluorescence (B) measurements, solutions contained 3 and 4 μM Rhodamine 800, respectively. In fluorescence measurements, spectra were recorded using λ_{ex}=660 nm.

The fluorescence emission spectra are presented in Fig. 2B. The fluorescence intensity varied markedly with the solvent, and decreased to less than one-fifth when the solvent was changed from acetone to water without a significant change of the emission peak. Table I summarizes the absorption maxima and relative fluorescence intensities of Rhodamine 800 dissolved in various organic solvents.

Effects of Rhodamine 800 on the Respiration Rate and RCR—We measured the RCR and respiration rate of isolated mitochondria while varying the concentration of Rhodamine 800 (Fig. 3). Concentrations below 5 μM had no significant effect on the mitochondrial respiration in state 3 or state 4, and therefore on RCR. Thus, we used ~5 μM Rhodamine 800 for the experiments.

Energy-Dependent Spectral Changes of Rhodamine 800 in Mitochondria—Figure 4 shows the absorption spectra of Rhodamine 800 incorporated into mitochondria in the presence and absence of an uncoupler, carbonyl cyanide *m*-chlorophenylhydrazone (CCCP). The absorption spectrum of the energized state (state 4) had absorption maxima at 706 and 648 nm, which were shifted to 690 and 628 nm by the addition of CCCP. The absorption peak at 706 nm of state 4 was not observed in several of the organic solvents tested. Addition of the uncoupler caused a blue shift of the absorption spectrum which resembled that in aqueous buffer solution (Fig. 2A). The difference absorption spectrum between energized state 4 and the non-energized uncoupled state showed broad absorption maxima at

TABLE I. **Absorption and emission maxima for Rhodamine 800 fluorescence in various organic solvents.** Each solvent contained 3 μM Rhodamine 800. Relative fluorescence intensity is expressed with reference to water.

Solvent	Dielectric constant (Debye)	Absorption maximum (nm)	Emission maximum (nm)	Relative fluorescence (%)
Water	1.9	687	692	100
Chloroform	1.1	685	694	660
Ethanol	1.7	691	695	470
Acetone	2.9	683	696	510
Acetonitrile	3.9	683	696	590
DMSO	4.5	696	706	230

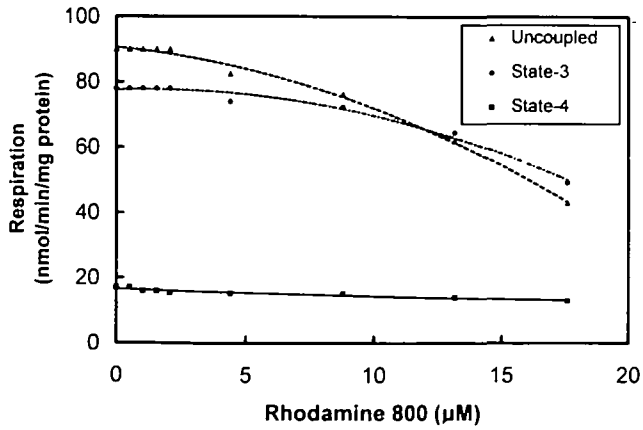

Fig. 3. **The effects of Rhodamine 800 on the respiration rate of mitochondria.** Oxygen consumption rates of mitochondrial suspension were measured in state 3, state 4, and the uncoupled state. Isolated mitochondria (0.5 mg protein/ml) were added to a reaction mixture consisting of 5 mM Tris-HCl, 0.25 M mannitol, 2.5 mM succinate, 2.5 mM KP_i, 10 mM KCl, 2.5 mM $MgCl_2$, 3 μM rotenone, and 1 mM EGTA (pH 7.4) at 25°C. Concentrations of ADP and CCCP were 200 and 2 μM for state 3 and the uncoupled state, respectively.

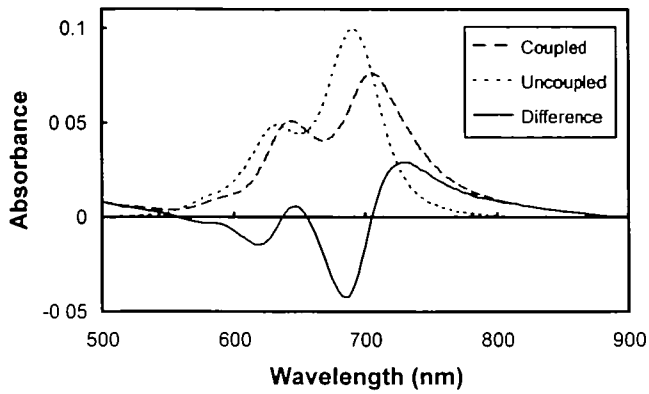

Fig. 4. **Absorption spectra of Rhodamine 800 in mitochondrial suspension.** Rat liver mitochondria (0.2 mg protein/ml) were incubated with 2.1 μM Rhodamine 800 in a reaction mixture consisting of 5 mM Tris-HCl, 0.25 M mannitol, 2.5 mM succinate, 2.5 mM KP_i, 10 mM KCl, 2.5 mM $MgCl_2$, 3 μM rotenone, and 1 mM EGTA (pH 7.4) at 25°C. Absorption spectra were recorded before (Coupled) and after (Uncoupled) the addition of 2 μM CCCP. The difference spectrum for coupled minus uncoupled was calculated manually.

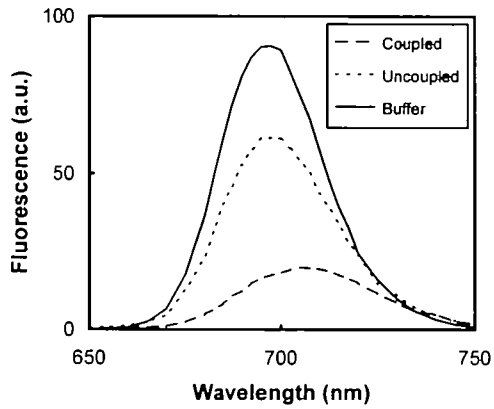

Fig. 5. **Fluorescence spectra of Rhodamine 800 in mitochondrial suspension.** Rat liver mitochondria (0.22 mg protein/ml) were incubated with 3 μM Rhodamine 800 in a reaction mixture consisting of 5 mM Tris-HCl, 0.25 M mannitol, 2.5 mM succinate, 2.5 mM KP_i, 10 mM KCl, 2.5 mM $MgCl_2$, 3 μM rotenone, and 1 mM EGTA (pH 7.4) at 25°C. Rhodamine 800 dissolved in the reaction mixture was also measured.

TABLE II. **Absorption and emission maxima for Rhodamine 800 fluorescence in mitochondrial suspension and hepatocytes.** Each suspension contained 3 μM Rhodamine 800. Relative fluorescence intensity is expressed with reference to aqueous buffer in Fig. 3.

Solution	Absorption maximum (nm)	Emission maximum (nm)	Relative fluorescence (%)
Buffer	687	692	100
Coupled mitochondria	705	710	22
Uncoupled mitochondria	690	693	71
Hepatocytes	704	709	29
Hepatocytes+CCCP	692	695	61

730 and 640 nm and minima at 685 and 630 nm, respectively. Thus, for dual-wavelength spectrophotometry, the absorbance difference at 730-685 nm was used in this study. The absorption difference at 730-800 nm was also used in some experiments, and gave identical results to those measured at 730-685 nm.

The effects of the energy states on the fluorescence spectra are shown in Fig. 5. The fluorescence intensity was very weak in the energized state 4, but was increased more than 3-fold in the non-energized uncoupled state. For comparison, the fluorescence spectrum in aqueous buffer solution, the emission intensity of which is larger than that of the uncoupled state, is also shown. The difference in the fluorescence spectra between energized and non-energized states was maximal at 710 nm, which was red-shifted from the value of 692 nm of the non-energized state (data not shown).

Table II summarizes the absorption peaks, fluorescence emission peaks and intensities of Rhodamine 800 in the isolated mitochondria in energized state 4 and non-energized uncoupled conditions, and those of hepatocytes are also presented. In the energized state of mitochondria, the fluorescence peak shifted from 692 to 710 nm, and the intensity decreased to 22% of that in aqueous solution. In

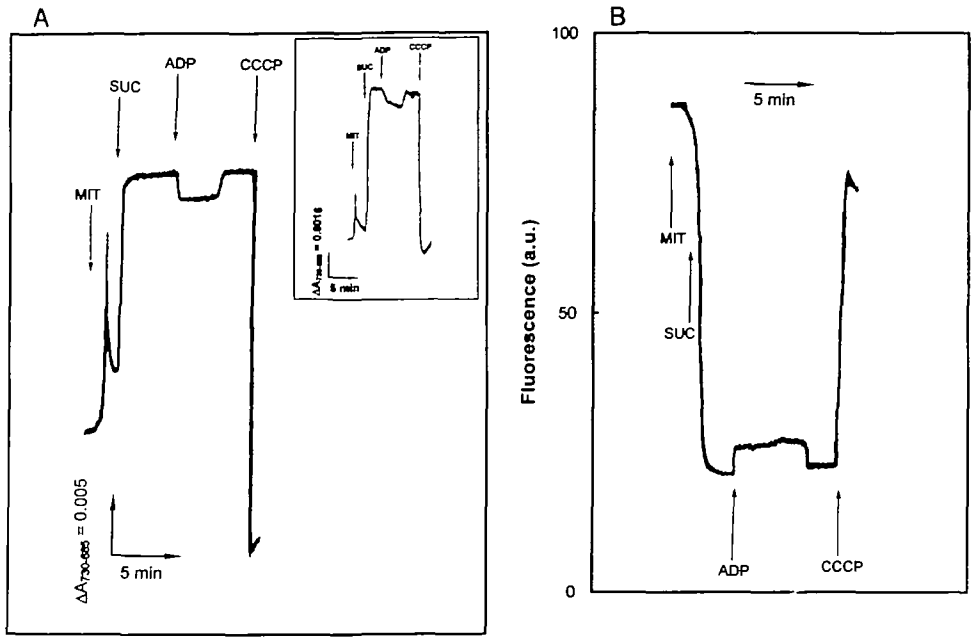

Fig. 6. **A: Absorption change of Rhodamine 800 in mitochondrial suspension with different energy states.** Absorbance at 730-685 nm was measured in a reaction mixture consisting of 5 mM Tris-HCl, 2.1 μM Rhodamine 800, 0.25 M mannitol, 2.5 mM KP_i, 10 mM KCl, 2.5 mM $MgCl_2$, 3 μM rotenone, and 1 mM EGTA (pH 7.4) at 25°C. Additions were 0.31 mg protein/ml mitochondria, 2.5 mM succinate, 200 μM ADP and 2 μM CCCP sequentially. The inset shows the absorbance measurements at 730-800 nm. **B: Fluorescence change of Rhodamine 800 in mitochondrial suspension.** Fluorescence excited at 660 nm (2 nm slit) and emitted at 692 nm (5 nm slit) was measured in a reaction mixture consisting of 5 mM Tris-HCl, 3 μM Rhodamine 800, and other components as described in the legend to (A). Additions were 0.22 mg protein/ml mitochondria, 2.5 mM succinate, 125 μM ADP, and 3 μM CCCP sequentially.

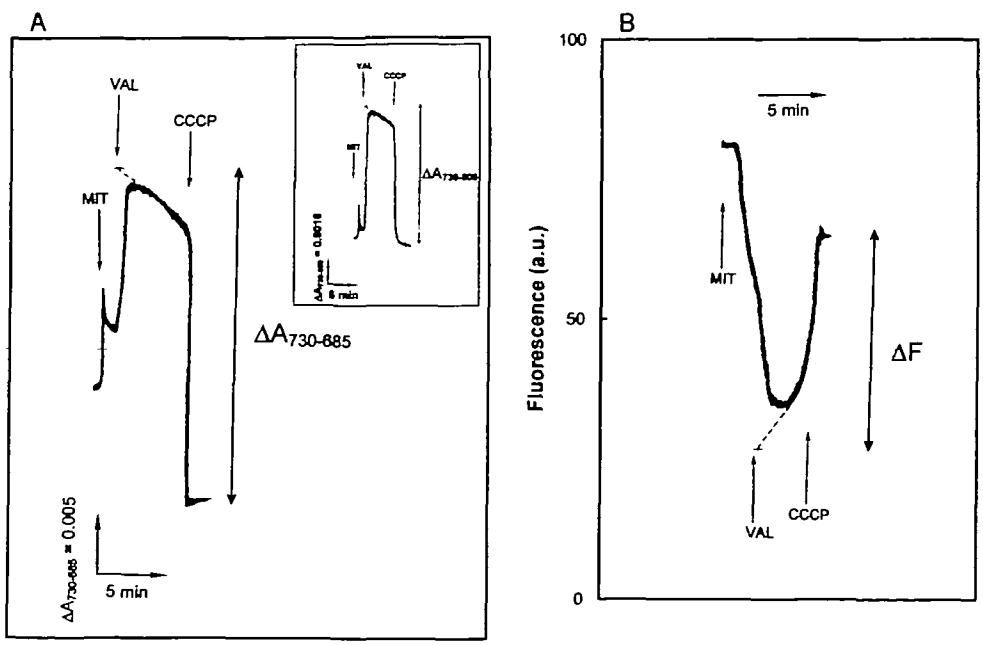

Fig. 7. **A: Absorbance change of Rhodamine 800 caused by potassium diffusion potential.** Absorbance was measured in a reaction mixture consisting of 5 mM Tris-HCl, 0.25 M mannitol, 2.5 mM NaP_i, 1 mM KCl, 2.5 mM $MgCl_2$, 3 μM rotenone, and 1 mM EGTA (pH 7.4) at 25°C. Additions were 0.31 mg protein/ml mitochondria, 30 nM valinomycin and 2 μM CCCP sequentially. The inset shows the absorbance changes of Rhodamine 800 at 730 minus 800 nm with a similar procedure. **B: Fluorescence change caused by potassium diffusion potential.** Fluorescence at 692 nm was measured in the reaction mixture as described in (A). Additions were 0.31 mg protein/ml mitochondria, 30 nM valinomycin, and 3 μM CCCP sequentially.

the non-energized state, the fluorescence peak shifted to 693 nm and the intensity recovered to about 70% of that in aqueous solution.

Optical Response of Rhodamine 800 in Mitochondria—Figure 6A shows the absorption changes of Rhodamine 800 incorporated into mitochondria under various respiratory conditions in which the absorption difference at 730-685 nm was measured. After the addition of mitochondria without an oxidizable substrate, the increase in absorption was relatively small due to the non-energized state 1 respiration. The addition of succinate caused an immediate, large increase of absorbance due to the energization of mitochondria in state 2 respiration. Subsequent addition of ADP caused a slight decrease in absorbance due to state 3 respiration. After the complete conversion of ADP to ATP, the absorption intensity increased again and returned to that of state 2. Thus, mitochondrial energy state in state 2 and state 4 was the same. Addition of the uncoupler CCCP caused a rapid and large decrease in absorbance. The inset shows the similar optical responses of Rhodamine 800 measured at 730-800 nm in the near-infrared range. Though the intensity of the absorption change was about 1/4 (Fig. 4), relative optical responses were nearly identical to those of 730-685 nm.

Fluorescence intensity changes in the various respiratory conditions are also presented in Fig. 6B, whose profiles are nearly mirror-images of the absorption measurements shown in Fig. 6A.

Relationship between the Optical Responses of Rhodamine 800 and $\Delta\Psi_K$—The absorption change of Rhodamine

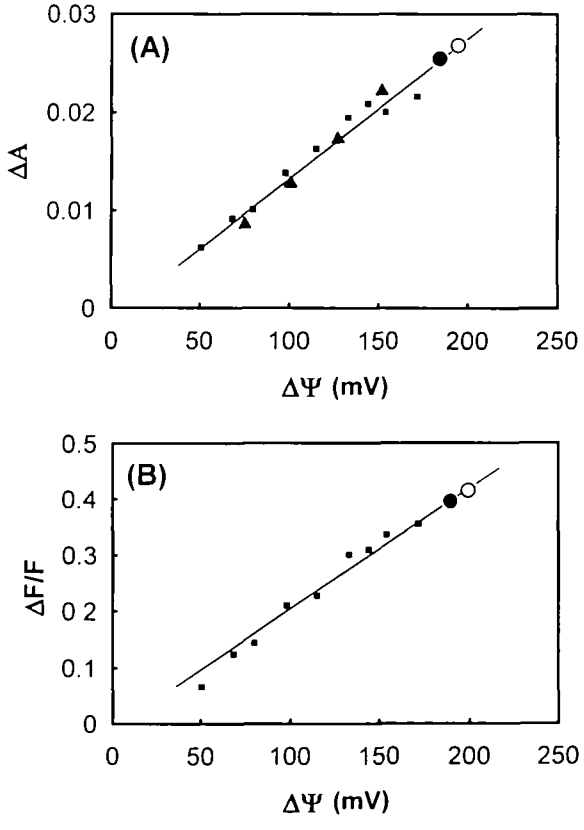

Fig. 8. **Relationship between absorption and fluorescence change of Rhodamine 800 and potassium diffusion potential in mitochondrial suspension.** In (A), ΔA was the difference between maximum and minimum, as described in the legend to Fig. 7. ▲ shows the value calculated from $\Delta A_{730-800}$ in Fig. 7A by multiplying by the appropriate coefficient. In (B), ΔF was as described in the legend to Fig. 7B, and F was the fluorescence obtained after the addition of CCCP. $\Delta\Psi_K$ was varied by varying KCl between 0.1 to 16 mM and other components were as described in the legend to Fig. 7A. ● and ○ show the extrapolated values of the membrane potential at state 3 and state 4, respectively.

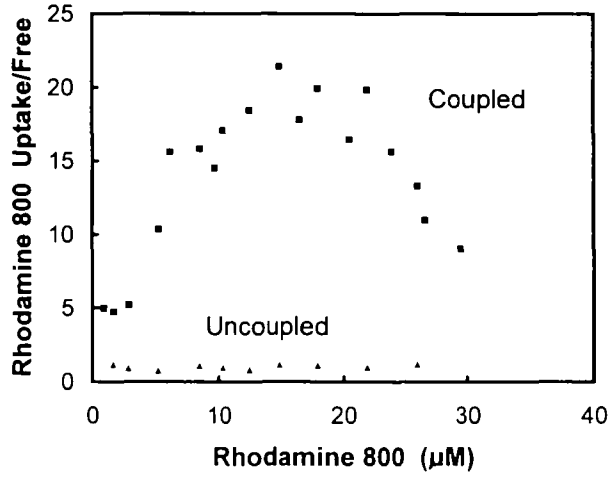

Fig. 9. **Mitochondrial uptake of Rhodamine 800 in coupled and uncoupled conditions.** Rat liver mitochondria, 0.59 mg protein/ml, were incubated with 0.8-29.4 μM Rhodamine 800 for 5 min at state 4 in a reaction mixture consisting of 5 mM Tris-HCl, 0.25 M mannitol, 2.5 mM succinate, 2.5 mM KP_i, 10 mM KCl, 2.5 mM $MgCl_2$, 3 μM rotenone, and 1 mM EGTA (pH 7.4) at 25°C. After incubation for 5 min, suspensions were centrifuged for 5 min at 5,000×g using a Himac-SCR 20B (Hitachi, Tokyo), and free Rhodamine 800 in the supernatant was determined from the absorbance at 685 nm. Accumulated Rhodamine 800 was considered to be total minus free Rhodamine.

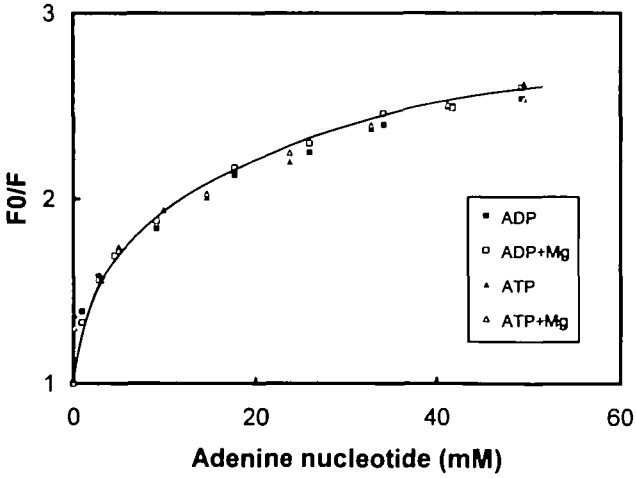

Fig. 10. **Stern-Volmer plot of fluorescence quenching of Rhodamine 800 by adenine nucleotide.** Fluorescence excited at 660 nm and emitted at 692 nm was measured in 5 mM Tris-HCl buffer containing 3 μM Rhodamine 800 and 0-50 mM ADP or ATP, in the presence and absence of 5 mM $MgCl_2$. The other components in the reaction mixture were as described in the legend to Fig. 3. F_0/F is the ratio of fluorescence in the absence of nucleotide to that in its presence.

800 is also related to the valinomycin-induced potassium diffusion potential, $\Delta\Psi_{K^+}$ (Fig. 7A). Formation of $\Delta\Psi_{K^+}$ required 15-30 s after the addition of valinomycin. After the initial increase of absorbance, the absorbance decreased gradually with the gradual decay of formed $\Delta\Psi_{K^+}$. Addition of CCCP caused the collapse of $\Delta\Psi_{K^+}$ and the absorbance decreased to the original level. Absorption change measured at 730-800 nm gave identical results (inset in Fig. 7A). The fluorescence response gave a similar result (Fig. 7B).

Changing the potassium concentration in the medium, we then systematically measured the valinomycin-induced absorption intensity of Rhodamine 800. Based on the Nernst equation (1), the relative absorption intensity of Rhodamine 800 was plotted against $\Delta\Psi_{K^+}$. As can be seen in Fig. 8A, the intensity was linearly related to $\Delta\Psi_{K^+}$. From Fig. 8A, we determined the membrane potentials of state 4 and state 3 to be 191 and 184 mV, respectively. Absorption intensity measured at 730-800 nm was also linearly related to $\Delta\Psi_{K^+}$. A linear relationship between the fluorescence intensity and $\Delta\Psi_{K^+}$ was also obtained, as shown in Fig. 8B. From Fig. 8B, membrane potentials of state 3 and state 4 were calculated to be 203 and 194 mV, respectively, slightly larger than those based on the absorbance measurements.

The similarity of the optical properties of Rhodamine 800 in non-energized mitochondria and aqueous buffer solution (Tables I and II) suggested that Rhodamine 800 might be incorporated into mitochondria in parallel with the membrane potential and be excluded from the mitochondria by uncoupling. This was confirmed by direct assay of the uptake of Rhodamine 800 in the mitochondria.

Figure 9 shows the concentration dependence of the uptake of Rhodamine 800 in the mitochondria. In state 4, the ratio of uptake/free Rhodamine was around 5-6 below 5 μM Rhodamine 800. Considering the mitochondrial space, the ratio of the concentration of Rhodamine 800 in mitochondria to that in the medium was 8000. This showed that about 83-86% of added Rhodamine 800 was incorporated into mitochondria. Increasing the amount of Rhodamine 800 resulted in an increase in the uptake/free ratio to ~20, where about 95% of added Rhodamine 800 was incorporated. As is observed in Fig. 3, the inhibition of the respiration by Rhodamine was almost negligible at 15 μM, and therefore the membrane potential was not affected by the Rhodamine. In contrast, at Rhodamine 800 concentrations above 15 μM, the ratio of uptake/free Rhodamine decreased almost linearly with the concentration, showing that the maximal incorporation of Rhodamine 800 occurred at around 15 μM.

With uncoupled mitochondria, the ratio of uptake/free Rhodamine was around 0.8-1.2, and was unchanged when the concentration of added Rhodamine 800 was changed from 2 to 30 μM. This showed that non-energized mito-

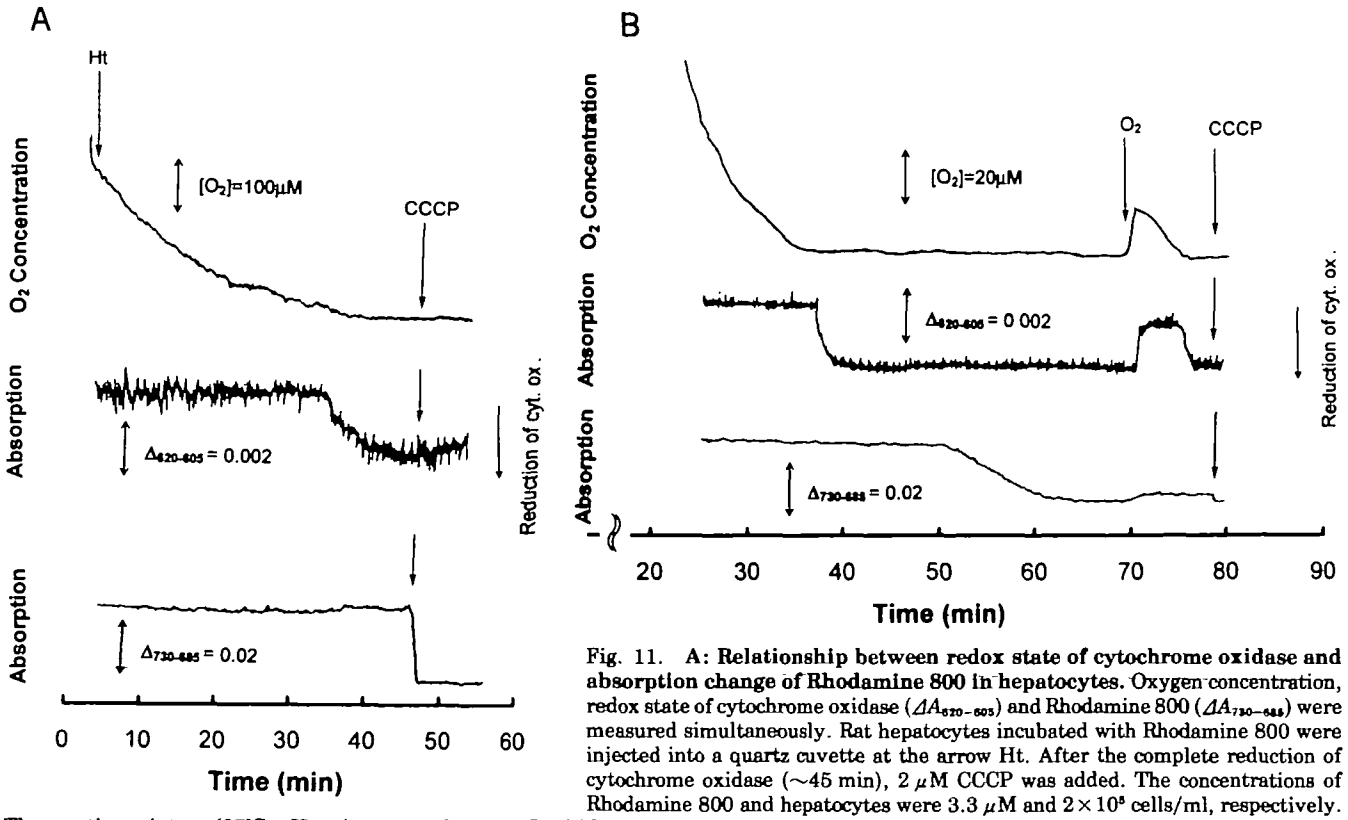

Fig. 11. **A: Relationship between redox state of cytochrome oxidase and absorption change of Rhodamine 800 in hepatocytes.** Oxygen concentration, redox state of cytochrome oxidase ($\Delta A_{620-605}$) and Rhodamine 800 ($\Delta A_{730-685}$) were measured simultaneously. Rat hepatocytes incubated with Rhodamine 800 were injected into a quartz cuvette at the arrow Ht. After the complete reduction of cytochrome oxidase (~45 min), 2 μM CCCP was added. The concentrations of Rhodamine 800 and hepatocytes were 3.3 μM and 2×10^8 cells/ml, respectively. The reaction mixture (37°C, pH 7.4) contained 10 mM HEPES, 139 mM NaCl, 3.57 mM $NaHCO_3$, 5.63 mM KCl, 1.42 mM $MgSO_4$, 1.43 mM KH_2PO_4, and 3.03 mM $CaCl_2$. **B: Effect of re-oxidation on the redox state of cytochrome oxidase and the absorption change of Rhodamine 800 in hepatocytes.** After the complete reduction of cytochrome oxidase (~40 min), the cuvette containing hepatocytes was left for 30 min, then the buffer containing hepatocytes was transiently re-oxidized by the addition of oxygen-saturated buffer solution (~10 μl, at arrow O_2). After the second reduction of cytochrome oxidase (~79 min), 2 μM CCCP was added. The concentrations of Rhodamine 800 and hepatocytes were 3.3 μM and 2×10^8 cells/ml, respectively, and other conditions were as described in the legend to (A).

chondria retained about half of added Rhodamine 800.

Fluorescence Quenching of Rhodamine 800 by Adenine Nucleotide—Figure 10 shows the fluorescence quenching of Rhodamine 800 by adenine nucleotide, ADP, and ATP in the presence and absence of Mg^{2+}. The Stern-Volmer plot of Fig. 10 did not give a straight line, a characteristic of dynamic quenching. The downward curvature was consistent with static quenching by adenine nucleotide (*21*). No difference between ADP and ATP was observed, and excess Mg^{2+} did not affect the quenching.

Isolated Hepatocytes—Figure 11A shows the absorption changes of Rhodamine 800 and cytochrome oxidase in isolated hepatocytes during the transition from aerobic to anaerobic conditions. Respiration caused the oxygen concentration to decrease to nearly zero, where cytochrome oxidase started to be reduced (~36 min). In anoxia, however, the absorbance of Rhodamine 800 measured at 730-685 nm was unchanged, but was decreased rapidly by the addition of CCCP (~45 min). Cytochrome oxidase did not show further reduction by CCCP. This indicated that, in the early stage of anoxia, hepatocytes were still in the energized state, even though the oxygen level fell to nearly zero. Figure 11B demonstrates the dissociation of the redox state of cytochrome oxidase and the energy state in anoxia.

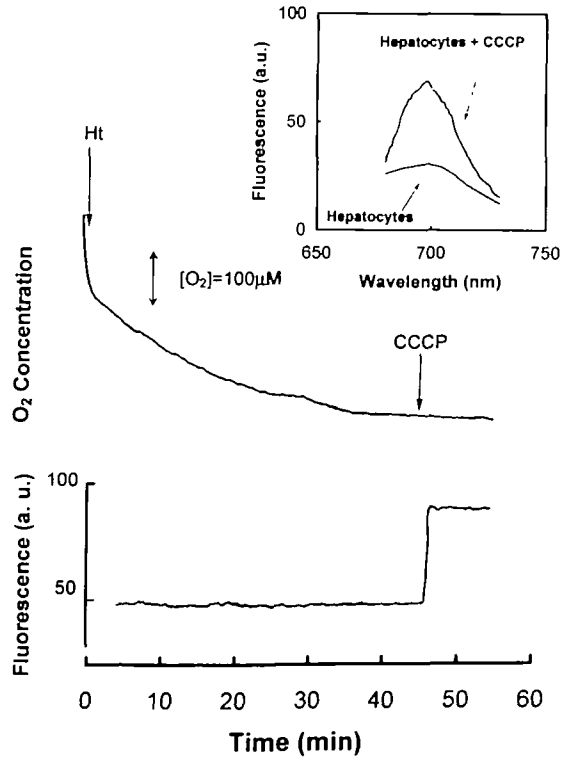

Fig. 12. **Fluorescence spectral change of Rhodamine 800 in rat hepatocytes.** The oxygen concentration and fluorescence intensity at $\lambda_{ex}=660$ nm were measured simultaneously. Rat hepatocytes, incubated with Rhodamine 800, were injected into the quartz cuvette at the arrow Ht. After the complete consumption of oxygen (~47 min), 2 μM CCCP was added. The concentrations of Rhodamine 800 and hepatocytes were 3.3 μM and 2×10^5 cells/ml, respectively, and other conditions were as described in the legend to Fig. 11A. Inset shows the fluorescence spectra of Rhodamine 800 incubated with rat hepatocytes excited at $\lambda_{ex}=660$ nm. Spectra were recorded before (Hepatocytes) and after (Hepatocytes+CCCP) the addition of 2 μM CCCP.

After the reduction of cytochrome oxidase in anoxia, the energy level of the hepatocytes (mitochondria) was maintained for ~5 min, then decreased gradually, as shown by the gradual decrease in Rhodamine 800 absorbance. The addition of a small amount of oxygen caused the re-oxidation of cytochrome oxidase, but the energy level did not recover.

Similar results were also obtained with fluorescence measurement (Fig. 12); no fluorescence change was observed in anoxia. Addition of CCCP caused a large increase in fluorescence intensity (~47 min). The inset shows the fluorescence emission spectra of Rhodamine 800 incorporated into the hepatocytes. Overall, the spectra resembled those of the isolated mitochondria in Fig. 5.

DISCUSSION

Optical Properties of Rhodamine 800—Though the chemical structure of Rhodamine 800 (Fig. 1) differs markedly from that of Rhodamine 123 (*6*), their optical properties resemble each other in general. As can be seen in Fig. 2 and Table I, the absorption and fluorescence emission spectra varied with the solvent used. These spectral changes could not be directly related to the polarity (dielectric constant) of the solvent (*22*), and, different from various other fluorescent dyes, the intensity was not related to the polarity of the solvent either. In addition, the excitation peak and emission peak were very close, with a maximum difference of only 10 nm. This relatively small Stokes shift of Rhodamine 800 as compared with that of Rhodamine 123 (excitation, 490 nm; emission, 530 nm) is due to its planar structure (*21*). Thus, fluorescence measurement of this dye requires special care to remove contamination by excitation light. We therefore used a cutoff filter inserted into the fluorometer.

When Rhodamine 800 was incubated with isolated mitochondria, an energy-dependent red shift of the absorbance and quenching of the fluorescence emission were observed. These spectral changes could be continuously monitored by dual-wavelength photometry and by fluorescence spectrophotometry at relatively longer wavelength in visible and near-infrared region. As can be seen in Fig. 8, the red shift and fluorescence quenching were linearly related to the valinomycin-induced potassium diffusion potential of $\Delta\Psi$. The sensitivity of fluorescence quenching to membrane potential was 2.3%/10 mV, similar to that of absorption measurement. Our estimated values of membrane potential at state 4 were slightly higher than generally reported values (~160 mV). Emaus *et al.*, however, gave a value of ~190 mV (*5*), similar to ours. Thus, the indirect method using the optical dye gives slightly higher values than those determined by a direct electrode method.

Adenine nucleotides also quenched the fluorescence (Fig. 10), and the potentials were the same with ATP and ADP, both with and without Mg^{2+}. This showed that fluorescence intensity changes observed in the various respiratory conditions were due to the changes of the mitochondrial energy state (membrane potential) rather than the changes of the concentration of ATP and ADP. This was confirmed by the information presented in Fig. 6, where state 2 and state 4 showed the same absorbance and fluorescence intensity. In addition, the concentration of ATP or ADP is about 1 mM in mitochondria, and the quenching is relative-

ly small compared to the quenching due to the change of membrane potential. The quenching by adenine nucleotide is static, involving a complex whose dissociation constant was about 1 mM, similar to that of Rhodamine 123 (*5*).

The uptake of Rhodamine 800 was concentration-dependent when mitochondria were in the energized state (Fig. 9). The ratio of the amount of uptake to free Rhodamine reached a maximum of 20 when the concentration of added Rhodamine 800 was about 15 μM. Considering the mitochondrial space, the concentration ratio inside and outside of the mitochondria became 8,000:1, twice as large as that of the other Rhodamine dye (*5*). At concentrations higher than 15 μM, the ratio decreased. This was due to the saturation of uptake into mitochondria. Thus, the K_m value of Rhodamine 800 was around 5 μM. In contrast, in the uncoupled non-energized state, the uptake/free Rhodamine ratio was almost constant at about 1, even when the concentration of Rhodamine 800 was increased to 30 μM. This meant that almost half of the dye was trapped inside the mitochondria. This incomplete release on uncoupling might have been due to the fact that this dye is more lipophilic than other cationic fluorescent dyes.

The largest difference of fluorescence intensity between energized and uncoupled conditions was obtained at around 15 μM Rhodamine 800; in other words, the highest sensitivity to the change of the energy state could be obtained at this concentration. However, as judged from the inhibition study shown in Fig. 3, the respiration rate and RCR started to decrease at concentrations higher than 5 μM. Therefore, we employed a dye concentration of around 5 μM in this study. At this concentration, the concentration ratio inside and outside mitochondria was still around 4,000:1. Thus, we selectively measured the absorption and fluorescence changes of the dye inside the mitochondria. The absorption and fluorescence changes could be followed with a good S/N ratio in the present study at this concentration (Fig. 11).

Near-Infrared Optical Staining for Energy State—Rhodamine 800 could be incorporated into mitochondria selectively in the hepatocytes. The similarity of the absorption and fluorescence spectra between isolated mitochondria and normal hepatocytes in the presence and absence of the uncoupler supported this conclusion. This was due to the fact that the both absorption and fluorescence were rather insensitive to the physicochemical properties of the solvent (Tables I and II), as Rhodamine 800 did not significantly change its optical properties when it bound nonspecifically to protein (unpublished observation). Thus, the dye in cytosol, released from mitochondria by uncoupling, gave optical spectra similar to that of the aqueous solution of mitochondrial suspension *in vitro*. The usefulness of Rhodamine 800 for evaluation of the tissue (cell) energy state was clearly demonstrated in aerobic-anaerobic transition where the oxygen concentration was also measured simultaneously in terms of the redox state of mitochondrial cytochrome. As can be seen in Fig. 11, in anoxia lower than 10^{-7} M oxygen (*23*), where cytochrome oxidase was completely reduced, mitochondria were in the fully energized state for ~5 min, as judged from Rhodamine 800 absorbance. Since the absorption change of Rhodamine 800 was 2%/10 mV, we could calculate the energy state quantitatively from the trace at various points. With isolated mitochondria in state 4, Rhodamine absorbance did not change for more than 10 min after the reduction of cytochrome oxidase in the anaerobic conditions. Schumacker *et al.* (*24*) reported that isolated hepatocytes prepared from the liver of non-starved rats, could survive up to 24 h under hypoxia (P_{O_2} = 18-22 Torr). Our conditions were completely anaerobic and starved. Therefore, the faster diminution of the membrane potential of mitochondria in hepatocytes was due to much higher energy consumption of the cells, in which glycolysis supported the energy demand for only a short period. After prolonged anoxia, addition of oxygen caused the full oxidation of cytochrome oxidase, but not recovery of mitochondrial membrane potential. This showed that hepatocytes could not recover upon re-introduction of oxygen after anoxia, after mitochondrial membrane potential had been lost. Thus, we could differentiate the failure of the energy state and oxygen supply of the cells.

For near-infrared spectrophotometry in clinical medicine, where the tissue oxygenation state due to hemoglobin oxygenation is measured non-invasively, the absorbance measurement of Rhodamine 800 at 730-800 nm can be used rather that at 730-685 nm, as shown in the present study (Figs. 6 and 11), since uncoupling of mitochondria caused a large change of light scattering, which is larger at the shorter wavelength of the visible region than in the near-infrared region. In Figs. 6 and 7, addition of uncoupler caused large decreases in absorbance, to below the original level. This was due to a scattering artifact, since, when measured at 730-800 nm in the near-infrared, the optical traces returned to the original levels. Thus, in addition to its high transparency, near-infrared measurement is less affected by the tissue scattering artifact. CuA in cytochrome oxidase in normal blood-circulating tissue (*11*) can be measured by using 805-830 nm absorbance instead of the 605-620 nm of heme $a+a_3$. Since all near-infrared spectrophotometers commercially available can measure absorption changes in the range from 700 to 900 nm, Rhodamine 800 can be used as a near-infrared active-energy-reporting dye. To apply it to *in vivo* blood-circulating conditions, however we must modify the chemical structure of Rhodamine 800, which might be more easily incorporated into the tissue by intravenous injection. An attempt to incorporate carboxyl ester groups into the dye is in progress.

A low concentration might not be harmful to living tissues (*cf.* Fig. 3). Our recent success with a hemoglobin-free perfused-rat-head model (*25*) supports the usefulness of this dye, in addition to fluorescence lifetime measurements (*26*). The results of those studies will be reported soon.

We conclude that Rhodamine 800 might be useful as an energy-reporting contrast agent (*27*) that can be employed in normal blood-circulation conditions for near-infrared spectrophotometry and imaging.

REFERENCES

1. Hirose, S., Yaginuma, N., and Inada, Y. (1974) Disruption of charge separation followed by that of the proton gradient in the mitochondrial membrane by CCCP. *J. Biochem.* **76**, 213-216
2. Laris, P.C., Bahr, D.P., and Chaffee, R.R.J. (1975) Membrane potentials in mitochondrial preparations as measured by means of a cyanine dye. *Biochim. Biophys. Acta* **376**, 415-425
3. Gear, A.R.L. (1974) Rhodamine 6G—A potent inhibitor of mitochondrial oxidative phosphorylation. *J. Biol. Chem.* **249**, 3628-3637

4. Higuti, T., Niimi, S., Saito, R., Nakasima, S., Ohe, T., Tani, I., and Yoshimura, T. (1980) Rhodamine 6G, inhibitor of both H^+-ejections from mitochondria energized with ATP and respiratory substrates. *Biochim. Biophys. Acta* **593**, 463-467
5. Emaus, R.K., Grunwald, R., and Lemasters, J.J. (1986) Rhodamine 123 as a transmembrane potential in isolated rat-liver mitochondria: spectral and metabolic properties. *Biochim. Biophys. Acta* **850**, 436-448
6. Millot, J., Sharonov, S., and Manfait, M. (1994) Scanning microspectrofluorometry of Rhodamine 123 in multidrug-resistant cells. *Cytometry* **17**, 50-58
7. Jöbsis, F.F. (1979) Oxidative metabolic effects of cerebral hypoxia. *Adv. Neurol.* **26**, 299-318
8. Kuroda, S., Houkin, K., Abe, H., Hoshi, Y., and Tamura, M. (1996) Near-infrared monitoring of cerebral oxygenation state during carotid endarterectomy. *Surg. Neurol.* **45**, 450-458
9. Seiyama, A., Hazeki, O., and Tamura, M. (1988) Noninvasive quantitative analysis of blood oxygenation in rat skeletal muscle. *J. Biochem.* **103**, 419-424
10. Nomura, Y. and Tamura, M. (1991) Quantitative analysis of the hemoglobin oxygenation state of rat brain *in vivo* by picosecond time-resolved spectrophotometry. *J. Biochem.* **109**, 455-461
11. Hoshi, Y. and Tamura, M. (1993) Dynamic changes in cerebral oxygenation in chemically induced seizures in rats. *Brain Res.* **603**, 215-221
12. Raue, R. and Harnisch, H. (1984) Dyestuff laser and light collectors—two new fields of application for fluorescent heterocycle compounds. *Heterocycles* **21**, 167-190
13. Shapiro, H.M. and Stephens, S. (1986) Flow cytometry of DNA content using oxazine 750 or related laser dyes with 633 nm excitation. *Cytometry* **7**, 107-110
14. Rizvi, N.H., Opalinska, M.M., French, P.M.W., and Tailor, J.R. (1991) A cw rhodamine 800 dye laser passively mode-locked with neocyanine. *Opt. Commun.* **80**, 57-59
15. Nakanishi, S. and Itoh, H. (1991) Subpicosecond photon echo quantum beats in a dye-doped polymer. *Jpn. J. Appl. Phys.* **30** No. 12A, L2042-2045
16. Seeger, S., Bachteler, G., Drexhage, K.H., Arden-Jacob, J., Deltau, G., Galla, K., Han, K.T., Müller, R., Köllner, M., Rumphorst, A., Sauer, M., Schulz, A., and Wolfrum, J. (1993) Biodiagnostics and polymer identification with multiplex dyes. *Ber. Bunsenges. Phys. Chem.* **97**, 1542-1548
17. Nedergaard, J. and Cannon, B. (1979) Preparation and properties of mitochondria from different sources in *Methods in Enzymology* (Fleischer, S. and Packer, L., eds.) Vol. 55, pp. 3-28, Academic Press, New York
18. Lowry, O.H., Rosebrough, N.J., Farr, A.L., and Randall, R.J. (1951) Protein measurements with the Folin phenol reagent. *J. Biol. Chem.* **193**, 265-275
19. Okajima, F. and Ui, M. (1982) Conversion of adrenergic regulation of glycogen phosphorylase and synthase from an α to β type during primary culture of rat hepatocytes. *Arch. Biochem. Biophys.* **213**, 658-668
20. Rossi, E. and Azzone, G.F. (1969) Ion transport in mitochondria —Energy barrier stoichiometry of aerobic K^+ translocation. *Eur. J. Biochem.* **7**, 418-426
21. Lakowitz, J.R. (1983) *Principles of Fluorescence Spectroscopy*, Plenum Press, New York and London
22. Stark, B. (1967) *Dipole Moments for Landolt-Boernstein Tables*, New Series, II/4, pp. 136-151, Springer, Berlin
23. Oshino, N., Sugano, T., Oshino, R., and Chance, B. (1974) Mitochondrial function under hypoxic conditions: the steady states of cytochrome $a+a_3$ and their relation to mitochondrial energy states. *Biochim. Biophys. Acta* **368**, 298-310
24. Schumacker, P.T., Chandel, N., and Agusti, A.N. (1993) Oxygen conformance of cellular respiration in hepatocytes. *Am. J. Physiol.* **265**, L395-402
25. Inagaki, M. and Tamura, M. (1993) Preparation and optical characteristics of hemoglobin free isolated perfused rat head *in situ*. *J. Biochem.* **113**, 650-657
26. Wakita, M., Nishimura, G., and Tamura, M. (1995) Some characteristics of the fluorescence lifetime of reduced pyridine nucleotide in isolated mitochondria, isolated hepatocytes and perfused rat liver *in situ*. *J. Biochem.* **118**, 1151-1161
27. Lakowitz, J.R. (1995) Lifetime based sensing. *SPIE Conference*, San Jose